



# Methane emissions due to reservoir flushing: a significant emission pathway?

Ole Lessmann<sup>1</sup>, Jorge Encinas Fernández<sup>1</sup>, Karla Martínez-Cruz<sup>1</sup>, Frank Peeters<sup>1</sup>

<sup>1</sup>Department of Biology, Limnological Institute, University of Konstanz, Konstanz, 78464, Germany

5 *Correspondence to:* Ole Lessmann (ole.lessmann@uni-konstanz.de); Frank Peeters (frank.peeters@uni-konstanz.de)

**Abstract.** Reservoirs can emit substantial amounts of the greenhouse gas methane (CH<sub>4</sub>) via different emission pathways. In some reservoirs, reservoir flushing is employed as a sediment management strategy to counteract growing sediment deposits that threaten reservoir capacity. Reservoir flushing utilizes the eroding force of water currents during water level drawdown to mobilize and transport sediment deposits through the dam outlet into the downstream river. During this process, CH<sub>4</sub> that is stored in the sediment can be released into the water and degas to the atmosphere resulting in CH<sub>4</sub> emissions. Here, we assess the significance of this CH<sub>4</sub> emission pathway and compare it to other CH<sub>4</sub> emission pathways from reservoirs. We measured seasonal and spatial CH<sub>4</sub> concentrations in the sediment of Schwarzenbach Reservoir, providing one of the largest datasets on CH<sub>4</sub> pore water concentrations in freshwater systems. Based on this dataset we determined CH<sub>4</sub> fluxes from the sediment and estimated potential CH<sub>4</sub> emissions due to reservoir flushing. CH<sub>4</sub> emissions due to one flushing operation can constitute 7–14% of the typical annual CH<sub>4</sub> emissions from Schwarzenbach Reservoir, whereby the amount of released CH<sub>4</sub> depends on the timing of the flushing operation within the season. The larger the thickness of the sediment layer mobilized during the flushing operation the larger the average CH<sub>4</sub> concentration per unit volume of flushed sediment. This suggests that regular flushing of smaller sediment layers releases less CH<sub>4</sub> than removal of the same sediment volume in fewer flushing events of thicker sediment layers. In other reservoirs with higher sediment loadings than Schwarzenbach Reservoir, reservoir flushing could cause substantial CH<sub>4</sub> emissions, especially when flushing operations are conducted frequently. Therefore, CH<sub>4</sub> emissions due to reservoir flushing must be included in estimates of annual overall greenhouse gas emissions from reservoirs that are subject to regular flushing operations.

## 1 Introduction

Worldwide ~16.7 million reservoirs exist (Lehner et al., 2011), and their number is projected to increase substantially in the near future (Zarfl et al., 2015) because of rising demand for hydropower. Besides being used for electricity generation and energy storage, reservoirs can serve multiple purposes such as water supply, flood control, irrigation and navigation (WCD (World Commission on Dams), 2000). In the past, hydropower was widely considered a greenhouse gas (GHG) neutral form of energy (Hoffert et al., 1998). Today, we know that the required reservoirs represent a significant source of GHG emissions, especially of the potent GHG methane (CH<sub>4</sub>), and researchers have estimated that reservoirs contribute around



30 17.7–70.0 Tg CH<sub>4</sub> to the annual global budget of atmospheric CH<sub>4</sub> (St. Louis et al., 2000; Bastviken et al., 2011; Deemer et al., 2016; Rosentreter et al., 2021).

CH<sub>4</sub> can be emitted from reservoirs via different pathways such as ebullition, plant-mediated transport, diffusion across the water-atmosphere interface, degassing during turbination (“drawdown flux”) and during spring or fall turnover as storage flux (Bastviken et al., 2011). CH<sub>4</sub> is typically produced in the anoxic part of the sediment (Le Mer and Roger, 2001).  
35 At oxic interfaces within the sediment, at the sediment surface or within the water column, CH<sub>4</sub> is at least partly oxidized by methane-oxidizing bacteria (Bastviken et al., 2002) before it reaches the water surface from where it is emitted as diffusive flux to the atmosphere. CH<sub>4</sub> flux via ebullition and plant-mediation, on the other hand, can bypass oxic interfaces, thus avoiding oxidation (Chanton and Whiting, 1995). In anoxic deep water of lakes and reservoirs, CH<sub>4</sub> typically accumulates and can reach large concentrations of stored CH<sub>4</sub> (Ragg et al., 2021). Intensive vertical mixing during spring and fall  
40 overturn causes rapid transport of the stored CH<sub>4</sub> to the water surface from where it diffuses to the atmosphere. This storage flux can substantially exceed the annual diffusive emissions during stratified conditions (Encinas Fernández et al., 2014).

While most of these emission pathways usually exist in both lakes and reservoirs, the drawdown flux of CH<sub>4</sub>, i.e., the degassing of CH<sub>4</sub> during turbination, occurs only in reservoirs where it can become the dominant source of CH<sub>4</sub> emissions (Kemenes et al., 2007), especially if the turbinated water is drawn from anoxic deep water where large amounts of  
45 CH<sub>4</sub> are stored. Ebullition of CH<sub>4</sub> is often observed as the dominant emission pathway, especially in shallow reservoirs (DelSontro et al., 2010; Sobek et al., 2012). It is well known that changes in hydrostatic pressure can induce bubble formation and release from sediments (Maeck et al., 2014; Harrison et al., 2017; Encinas Fernández et al., 2020). Therefore, water level drawdowns in reservoirs can substantially increase the ebullition flux of CH<sub>4</sub> due to decreasing pressure, which can become particularly large during fall drawdown or occur regularly during diel pumped-storage operations (Harrison et al., 2017; Encinas Fernández et al., 2020).  
50

Growing sediment deposits in reservoirs, caused by particles introduced from the catchment and organic matter produced within the system, pose a challenge to maintaining reservoir capacity (e.g., by decreasing reservoir storage volume). Globally, reservoir storage capacity is decreasing and is estimated to be completely lost for most reservoirs within 200–300 years if sediment management strategies are not adopted (ICOLD, 2009). Sediment management strategies are  
55 applied in reservoirs to reduce sediment yield, route sediments or remove already deposited sediment (Morris, 2020; Petkovšek et al., 2020). Deposited sediment can be removed by mechanical removal (e.g., dredging) or hydraulic flushing, which utilizes the eroding force of water currents during water level drawdown. The sediment is then mobilized in the water and transported through a dam outlet to the downstream river section. Consequently, any CH<sub>4</sub> previously stored in the sediment pore water is also mobilized into the water stream and can eventually degas to the atmosphere at the reservoir  
60 surface, during turbination, or downstream of the reservoir, leading to CH<sub>4</sub> emissions. In order to assess the relative importance of CH<sub>4</sub> emissions due to reservoir flushing compared to other typical CH<sub>4</sub> emission pathways, it is important to consider reservoir flushing frequency and sediment flushing volume. Among reservoirs with relatively regular flushing operations, flushing frequencies between twice a year and once every five years have been reported (Brandt and Swenning,



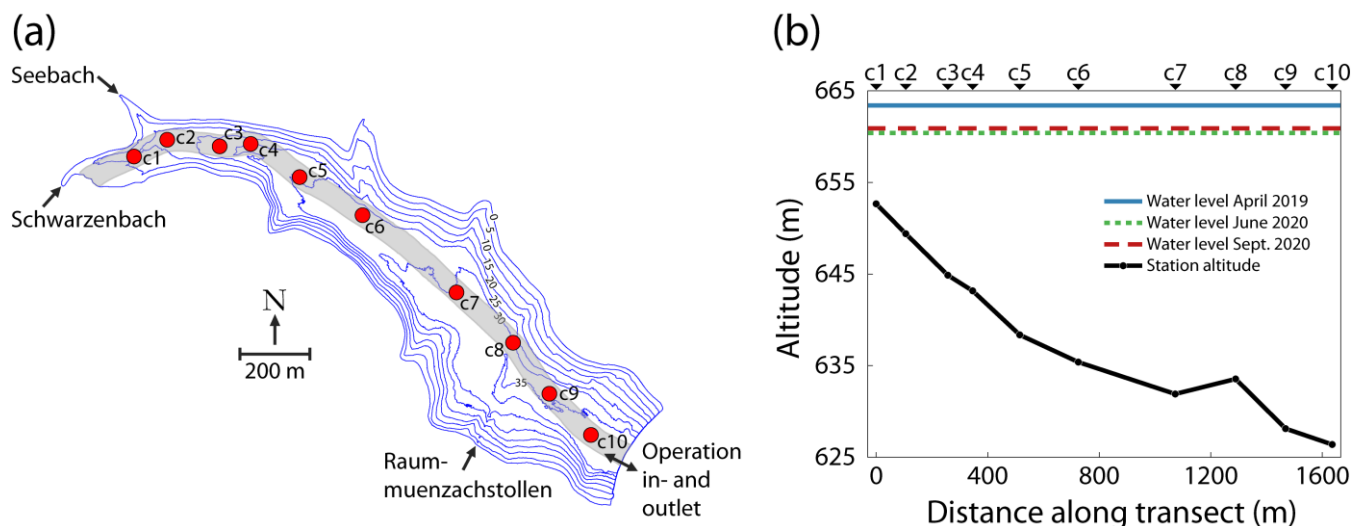
1999; Chang et al., 2003; Kantoush and Sumi, 2010; Fruchard and Camenen, 2012; Grimardias et al., 2017; Sumi et al.,  
65 2017; Antoine et al., 2020), but there are also reservoirs that are flushed irregularly (Sumi et al., 2017). Reservoirs with  
higher sedimentation rates need to be flushed more frequently than others. For instance, the Tapu reservoir in Taiwan is  
characterized by high sedimentation rates induced by heavy rainfalls and steep-sloped mountains and was flushed 10 times  
between 1991 and 1996 (Chang et al., 2003). The success of the reservoir flushing operation can be measured by the volume  
of sediment removed from the reservoir, which depends on reservoir geometry, sediment characteristics and operation  
70 strategy (Morris, 2020; Petkovšek et al., 2020).

In this study, we investigated CH<sub>4</sub> emissions due to reservoir flushing, a pathway that has not yet been included in  
estimates of CH<sub>4</sub> emissions from reservoirs. We determined the amount of CH<sub>4</sub> stored in the sediment pore water of a  
reservoir at different seasons and estimated potential CH<sub>4</sub> emissions resulting from reservoir flushing scenarios.  
Furthermore, we assessed the relative importance of reservoir flushing in comparison to other typical CH<sub>4</sub> emission pathways  
75 in reservoirs.

## 2 Material and methods

### 2.1 Study Site

Field measurements were conducted in Schwarzenbach Reservoir, which is located in the northern part of the Black Forest in  
southwest Germany (48°39.334'N, 8°19.630'E) at ~660 m above sea level (a.s.l.). The reservoir is operated as a pumped-  
80 storage hydroelectric energy system. At a maximum storage capacity of  $14.4 \times 10^6$  m<sup>3</sup>, the reservoir is 47 m deep and covers  
a surface area of ~0.66 km<sup>2</sup>. The reservoir's alkalinity and salinity are typically in the order of 0.3 mmol<sub>eq</sub> L<sup>-1</sup> and 0.04 g kg<sup>-1</sup>,  
respectively. The reservoir receives input from two natural creeks (Schwarzenbach and Seebach) located at the western end  
of the basin and from an artificial channel in the south (Raummuenzachstollen) that collects water from the immediate  
catchment area (Fig. 1a). Due to a sediment trap located upstream of the artificial channel, the Seebach and Schwarzenbach  
85 are the only sources for sediment transport into the reservoir. For the pumped-storage operation, an in- and outlet is based  
near the dam at ~5 m above ground. The contributions of the individual inputs are described in Mouris et al. (2018).



90 **Figure 1. (a) Bathymetric map of Schwarzenbach Reservoir showing in- and outflows and the position of the sampling stations (c1 – c10). The grey shaded area symbolizes the estimated basin-wide erosion channel with a 60 m width. (b) Sediment altitude at the sampling stations and water level during three field campaigns (April 2019, June 2020, and September 2020). The individual sampling stations are indicated above the panel.**

## 2.2 Field measurements

Three field campaigns (April 2019, June 2020 and September 2020) were conducted at Schwarzenbach Reservoir, during which a total of 47 sediment cores were retrieved, i.e., 13 in April 2019 and 17 in each of the campaigns in June and September. The sediment cores were sampled along the transect close to the thalweg (Fig. 1a). At each sampling station, two sediment cores were retrieved, except for station c5 in April 2019 and June 2020, and station c3 in September 2020, where only one sediment core was retrieved. The transect length was ~1.6 km, and the altitude of the sediment cores ranged between 626.4 and 652.7 m (Fig. 1b). In April 2019, the reservoir's water level was around 3 m higher than in June and September 2020. In April 2019, sediment cores were taken at station c1, c2, c4, c5, c6, c7 and c9 and in June and September 2020 at station c1, c2, c3, c5, c6, c7, c8, c9 and c10. Vertical temperature and dissolved oxygen (DO) profiles were measured in the water column at the respective stations with a multiparameter probe (CTD probe, RBR Ltd., Ottawa, Canada, equipped with a temperature and oxygen optode RBRcoda T.ODO fast). The temperature of the water overlaying the sediment (~0.5 m above the sediment surface) served as a proxy for the sediment temperature. Water samples for CH<sub>4</sub> analysis were taken using a 2-L water sampler (Limnos, Finland).

## 105 2.3. Measurements of CH<sub>4</sub> concentrations

Sediment cores were taken with a gravity corer equipped with a PVC liner of 600 mm length and an inner diameter of 58 mm. The liner was capped using a rubber stopper or a liner cap. Within 1–3 hours after sampling, the sediment cores were processed at the nearest shore. Sediment subsamples were taken through 0.6 cm pre-drilled holes (1 cm vertical spacing) in the PVC liner using 1 ml cutoff syringes at sediment depths of: 0.25, 1.25, 2.25, 3.25, 4.25, 5.25, 7.25, 10.25 and 15.25 cm.



110 Each sediment subsample was immediately inserted into a 100 ml glass bottle (DWK Life Science GmbH, Germany). The  
glass bottles were filled completely with demineralized water and closed using a PTFE-coated silicone septum (DWK Life  
Science GmbH, Germany). The bottle was shaken vigorously, enabling the pore water to dissolve into the water. The  
procedure to measure the CH<sub>4</sub> concentration in the water was adapted from Hofmann et al. (2010). Briefly, 50 ml liquid was  
sampled with a 50 ml syringe sediment settling and injected into a 100 ml glass injection vial (DWK Life Science GmbH,  
115 Germany) containing, 20–30 g of NaCl ( ≥ 99,5 %, p.a., ACS, ISO, Carl Roth GmbH, Germany) and 30–40 ml of  
demineralized water. After sample injection, the CH<sub>4</sub> degassed into the headspace (~35 ml) due to the oversaturated NaCl  
solution. The bottles were stored upside down until further processing to prevent CH<sub>4</sub> loss over time through the septum. The  
CH<sub>4</sub> concentration in the equilibrated headspace of the injection vial was measured using a gas chromatograph equipped with  
a flame ionization detector (GC 6000, Carlo Erba Instruments, UK). The CH<sub>4</sub> concentration in the water sample was  
120 obtained by referring the measured CH<sub>4</sub> concentration in the headspace to the volume of the respective water sample. With  
the concentration of CH<sub>4</sub> in the water sample  $C_{CH_4,ws}$ , the volume of the glass bottle  $V_{gb}$ , the volume of the sediment sample  
 $V_{ss}$ , the volume of the pore water  $V_{pw}$  and the porosity  $\phi$ , the concentration of CH<sub>4</sub> per sediment volume  $C_{CH_4,sed}$  and the  
concentration of CH<sub>4</sub> in the pore water  $C_{CH_4,pw}$  were calculated as:

$$C_{CH_4,sed} = \frac{C_{CH_4,ws} * (V_{gb} - (V_{ss} - V_{pw}))}{V_{ss}} \quad (\text{mmol L}^{-1}) \quad (1)$$

$$125 \quad C_{CH_4,pw} = \frac{C_{CH_4,sed}}{\phi} \quad (\text{mmol L}^{-1}) \quad (2).$$

The porosity of the sediment describes the ratio of void volume that is occupied by the pore water, to the total volume  
(Brimhall and Dietrich, 1987) and was calculated for each sediment subsample accordingly:

$$\phi = \frac{V_{pw}}{V_{ss}} \quad (-) \quad (3).$$

130 However, because the difference between  $V_{ss}$  and  $V_{pw}$  was small, the uncertainty of the volume ratios determined from  
weight measurements was rather large for individual sediment samples from specific depth and location. Therefore, we  
determined the average vertical profile of porosity in the sediment by fitting a cubic function of depth to all porosity profiles  
from all sampling campaigns (Fig. S1). The porosities of this average porosity profile were used to calculate the pore water  
concentrations  $C_{CH_4,pw}$ . Vertical profiles of  $C_{CH_4,pw}$  were obtained by measuring at sediment depths between 0.25 and 15.25  
cm. Missing data were estimated by bilinear interpolation of the CH<sub>4</sub> distribution. Missing values at boundaries were  
135 estimated by extrapolation, assuming constant concentrations below the depth of the deepest available measurement. Inter-  
and extrapolated values constituted ~10% of all data points.

#### 2.4. Diffusive CH<sub>4</sub> flux from the sediment into the water column

Assuming molecular diffusion within the sediment and using Fick's first law of diffusion accounting for the porosity and the  
tortuosity of the sediment, the vertical flux of CH<sub>4</sub> in the sediment is given by Berner (1980):

$$140 \quad F_{sed} = -\phi(D_{CH_4} \theta^{-2}) \frac{\partial C}{\partial z} \quad (\text{mmol m}^{-2} \text{ d}^{-1}) \quad (4)$$



where  $D_{CH_4}$  is the molecular diffusivity of  $CH_4$  in water ( $m^2 d^{-1}$ ),  $\phi$  is the porosity (-),  $\theta$  is the tortuosity (-), and  $\partial C/\partial z$  is the vertical gradient of the  $CH_4$  pore water concentration ( $mmol m^{-3}$ ). The diffusive flux of  $CH_4$  at the sediment-water interface,  $F_{sed}$  ( $mmol m^{-2} d^{-1}$ ), was assumed to correspond to the diffusive flux of  $CH_4$  in the uppermost part of the sediment (see also Berner 1980) and was determined using the gradient of the  $CH_4$  pore water concentration obtained by linear regression of the

145  $C_{CH_4,pw}$  from 0.25 cm, 1.25 cm, and 2.25 cm depth in the respective sediment core.  $D_{CH_4}$  was calculated from the Schmidt number of  $CH_4$  (Wanninkhof, 1992) and the viscosity of the water (Weast, 1988), taking temperature and salinity into account. We assumed the sediment's temperature and salinity were the same as in the water overlaying the sediment. As porosity, we used the median of the porosity measurements in the upper 2.25 cm of all sediment cores ( $\phi=0.97$ ). The tortuosity was determined using the porosity according to Boudreau (1997):

$$150 \quad \theta^2 = 1 - \ln(\phi^2) \quad (-) \quad (5).$$

## 2.5. Stored $CH_4$ in the potentially eroded sediment volume due to reservoir flushing

For the estimation of the  $CH_4$  storage in the sediment, missing values in the measured profiles of  $C_{CH_4, sed}$  were estimated by inter- and extrapolation using the same procedure as in the case of  $C_{CH_4,pw}$ . Additionally, profiles of  $C_{CH_4, sed}$  were extended to 100 cm sediment depth assuming that  $C_{CH_4, sed}$  below 15 cm sediment depth is constant. Finally, the profiles of  $C_{CH_4, sed}$  were

155 linearly interpolated to obtain a regular 1 cm vertical resolution starting at 0.5 cm sediment depth. From these profiles, the total amount of  $CH_4$  stored at different depths within the sediments of Schwarzenbach Reservoir was calculated by lateral and vertical integration.

Based on reported channel widths during reservoir flushing from a similar-sized reservoir (Kantoush et al., 2010), the eroded sediment surface area was assumed to correspond to a 60 m wide flushing channel along the thalweg of

160 Schwarzenbach Reservoir (Fig. 1a). The total surface area covered by this channel was about  $1.1 \times 10^5 m^2$ . We assumed that the  $CH_4$  profile from a sampling station represents the  $CH_4$  concentrations also in the sediment in the proximity of the sampling station. Respective sediment areas were calculated by extending laterally to the half distance of bordering stations. For the outermost stations, sediment areas extended to the respective end of the basin. With all stations representing complementary parts of the total sediment surface area,  $C_{CH_4, sed}$  profiles measured at the different stations and their

165 corresponding sediment areas were used to calculate the amount of  $CH_4$  stored per unit depth at different sediment depths across the entire channel,  $S_{CH_4}$  ( $mmol m^{-1}$ ). The average concentration and the total amount of  $CH_4$  in the potentially eroded sediment volume due to reservoir flushing ( $C_{CH_4, FSL}$  ( $mol m^{-3}$ ) and  $N_{CH_4, FSL}$  (mol), respectively) depends on the thickness of the flushed sediment layer.  $N_{CH_4, FSL}$  was estimated from the stored methane  $S_{CH_4}$  by integrating vertically down to the depth of sediment erosion during flushing ( $Z_e$ ):

$$170 \quad N_{CH_4, FSL}(Z_e) = \int_0^{Z_e} S_{CH_4}(z') dz' \quad (mol) \quad (6).$$

$C_{CH_4, FSL}$  was obtained by dividing  $N_{CH_4, FSL}$  with the volume of mobilized sediment.



The relevance of  $N_{CH_4,FSL}$  for overall  $CH_4$  emissions from Schwarzenbach Reservoir was assessed by comparing the  $N_{CH_4,FSL}$  stored in the potentially eroded sediment volume during a flushing event with other pathways of  $CH_4$  emission from Schwarzenbach Reservoir (ebullition, diffusive  $CH_4$  emissions from the reservoir surface, and degassing during turbinaton).

## 175 3 Results

### 3.1 Reservoir characterization

Schwarzenbach Reservoir is a pumped-storage system, and reservoir management can substantially change the water level. In April 2019, water levels were about 3 m higher than in June and September 2020 (Fig. 1b). The water column of Schwarzenbach Reservoir was stably stratified during all three campaigns (Fig. 2a). In June and September 2020, DO concentrations were oversaturated near the water surface and above  $2 \text{ mg L}^{-1}$  throughout the entire water column (Fig. 2b). In April 2019 the DO sensor failed, but DO concentrations can be expected to be around  $10 \text{ mg L}^{-1}$  as is indicated by a DO profile measured in April 2018. (Fig. 2b).

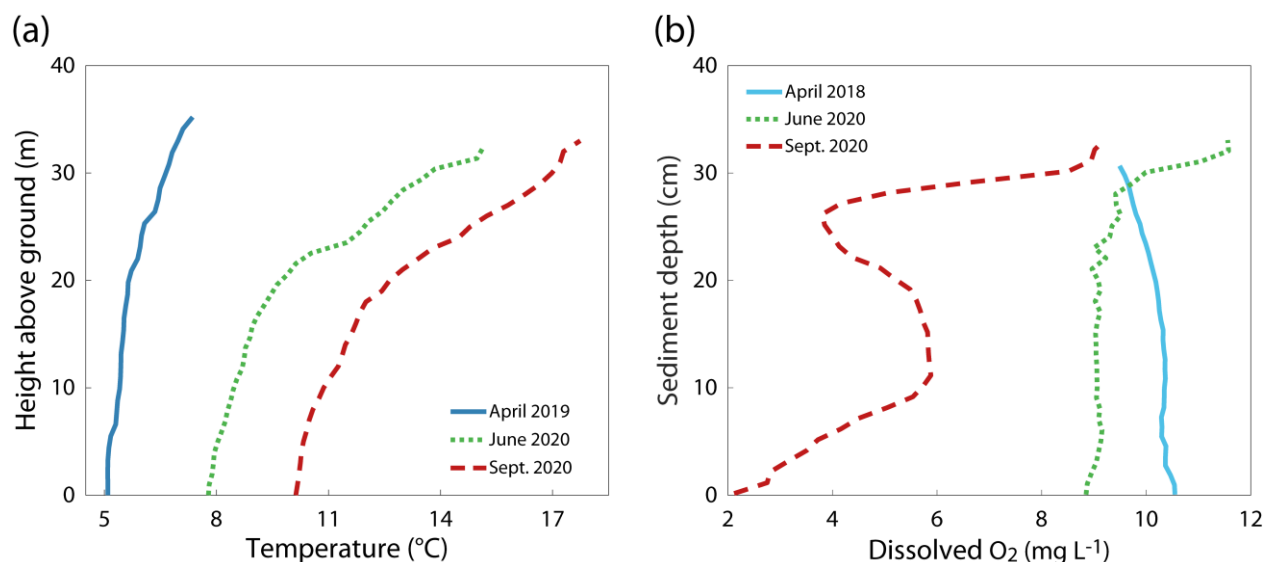


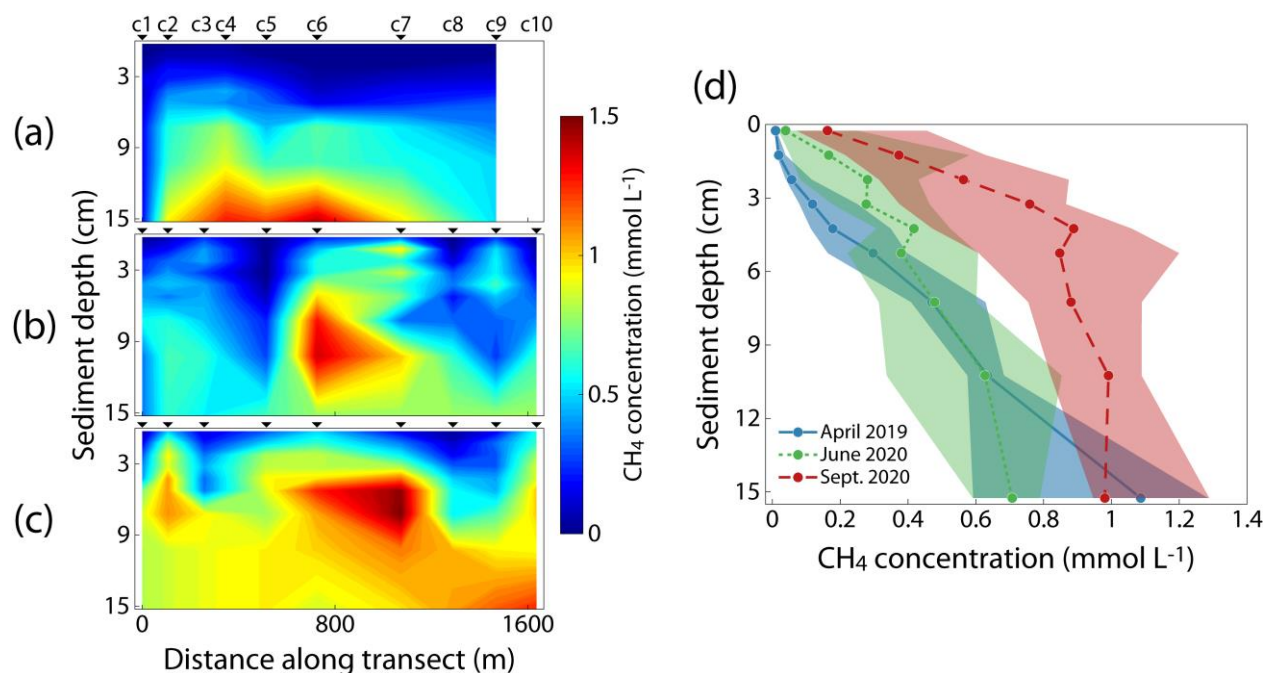
**Figure 2. Profiles of (a) temperature and (b) dissolved oxygen at station c9 during different seasons in Schwarzenbach Reservoir.**

### 185 3.2 Spatiotemporal dynamics of $CH_4$ in sediment pore water

The  $CH_4$  concentrations in the pore water of the sediment of the reservoir differed spatially and seasonally (Fig. 3). In April 2019 and June 2020, regions with particularly large  $CH_4$  concentrations were located in the center of the transect at deep sediment layers, whereas at the same depth within the sediment,  $CH_4$  concentrations near the dam and the western end of the basin were considerably lower (Fig. 3a–b). In September 2020, the largest  $CH_4$  concentrations were still found in the middle of the transect but were, in general more evenly distributed across the transect and larger at shallower depth than in June 2020 (Fig. 3c). For each sampling campaign, we determined a median  $CH_4$  pore water profile by compiling the medians of



all measurements from the same sediment depth into a vertical profile (Fig. 3d). With the progressing season, we observed an increase in median CH<sub>4</sub> pore water concentrations and stronger vertical CH<sub>4</sub> gradients in the upmost 5 cm of the sediment. In April 2019, the median CH<sub>4</sub> concentration profile was characterized by relatively low concentrations and a weak vertical gradient in the upper sediment layers, followed by an almost linear increase in CH<sub>4</sub> concentrations. In contrast, the median CH<sub>4</sub> profiles in June and September 2020 both showed stronger gradients in the upper sediment layers with a more saturated curve in deeper layers. However, in September 2020, the overall CH<sub>4</sub> concentrations were much larger in all but the deepest sampled sediment layers. The mean and median CH<sub>4</sub> concentration across all measurements in April 2019 were 0.27 mmol L<sup>-1</sup> and 0.16 mmol L<sup>-1</sup>, in June 2020 0.37 mmol L<sup>-1</sup> and 0.34 mmol L<sup>-1</sup>, and in September 2020 0.63 mmol L<sup>-1</sup> and 0.68 mmol L<sup>-1</sup>, respectively, indicating an increase of overall CH<sub>4</sub> concentration in the pore water with the progressing season.

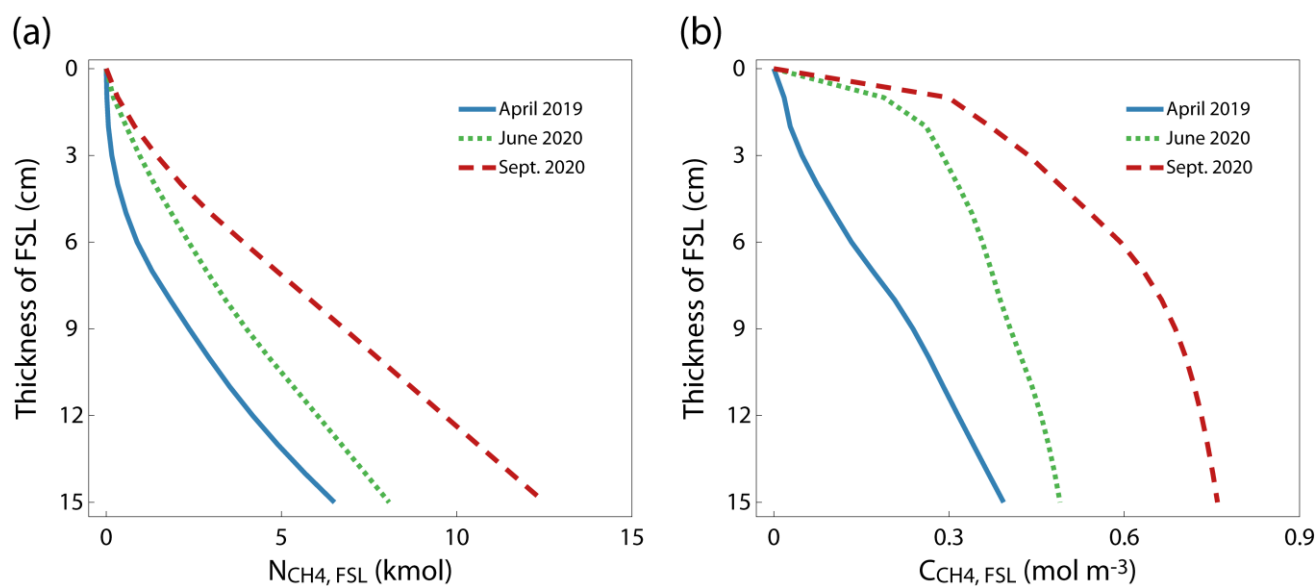


205 **Figure 3.** (a–c) Spatial distribution of CH<sub>4</sub> pore water concentration in the top 15 cm of the sediment along the transect in April 2019 (a), June 2020 (b) and September 2020 (c). The individual sampling stations are indicated above the panels. d) Median CH<sub>4</sub> concentration of all pore water profiles within each campaign. Shaded areas display the 25<sup>th</sup> and 75<sup>th</sup> percentile.

### 3.3 CH<sub>4</sub> storage estimation

To estimate the stored CH<sub>4</sub> that is potentially emitted due to sediment erosion during reservoir flushing of Schwarzenbach Reservoir, we calculated  $N_{CH_4,FSL}$ , the amount of CH<sub>4</sub> stored between the top of the sediment and a hypothetical erosion depth within the 60 m wide erosion channel centered around the thalweg along the basin (Fig. 4, the channel is indicated in Fig. 1a). With the progressing season,  $N_{CH_4,FSL}$  was consistently higher at all erosion depths. Assuming an erosion depth of 15 cm,  $N_{CH_4,FSL}$  was 6.5, 8.1 and 12.5 kmol CH<sub>4</sub> in April 2019, June 2020 and September 2020, respectively.

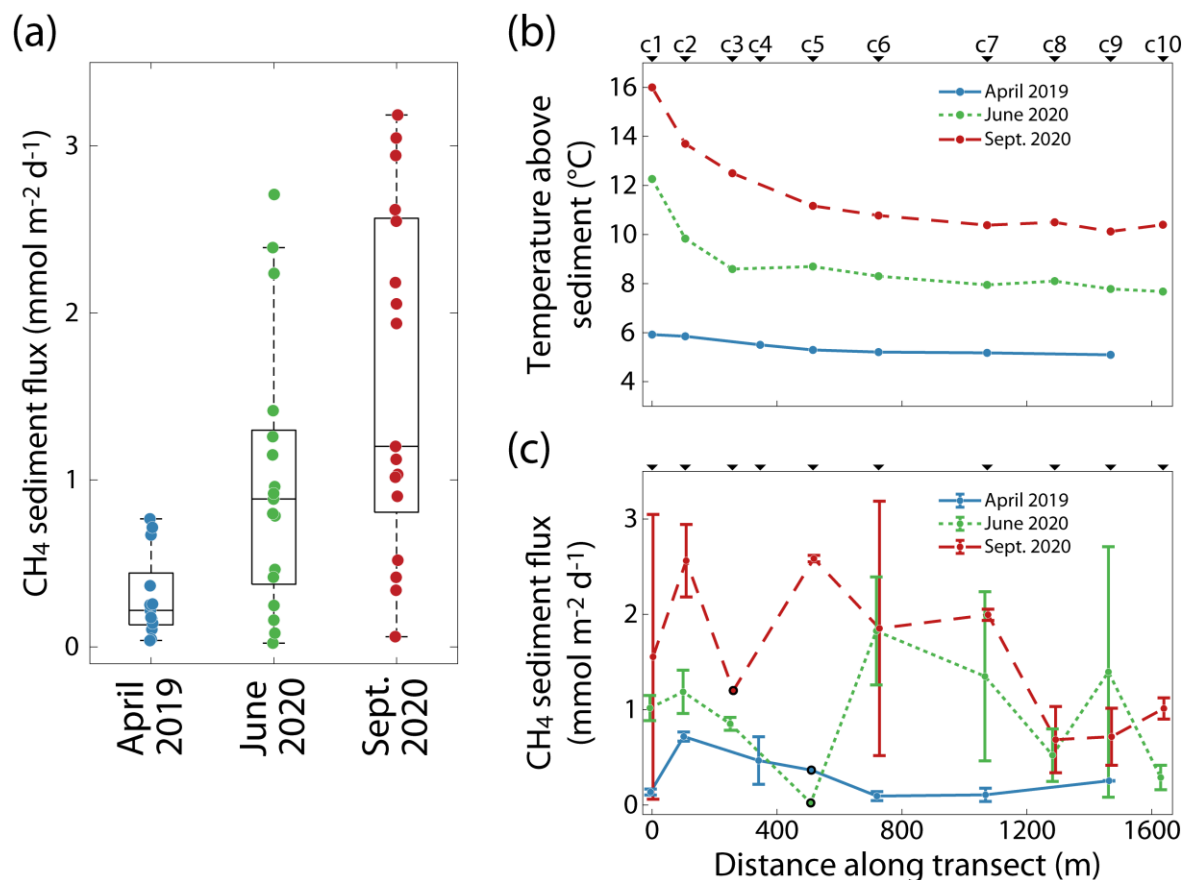




215 **Figure 4. (a) Stored amount of CH<sub>4</sub> in the flushed sediment layer,  $N_{CH_4,FSL}$ , as a function of layer thickness. The thickness of the flushed sediment layer corresponds to the erosion depth of the sediment in the 60 m wide erosion channel. (b) The average CH<sub>4</sub> concentration in the flushed sediment layer.**

### 3.4 CH<sub>4</sub> fluxes at the sediment-water interface

Diffusive CH<sub>4</sub> fluxes at the sediment-water interface  $F_{sed}$  were determined for each campaign at each station along the transect (Fig. 5c). The overall variability of  $F_{sed}$  from all stations measured during a campaign increased with the progressing  
220 season from April to September (Fig. 5a). Compared to the range of  $F_{sed}$  in April 2019, the range of  $F_{sed}$  was ~3.5 times larger in June 2020 and ~4 times larger in September 2020. While the lowest measured  $F_{sed}$  were very similar across the three campaigns (between 0.02 and 0.06 mmol m<sup>-2</sup> d<sup>-1</sup>), the median and maximum CH<sub>4</sub> fluxes increased from April to September. The average CH<sub>4</sub> flux over all measurements was 1.02 mmol m<sup>-2</sup> d<sup>-1</sup>. Sediment temperatures, approximated by water temperature ~0.5 m above the sediment, increased with the season (Fig. 5b). In April 2019, the temperatures along the  
225 transect were rather uniform, ranging between 5.1 °C (c9) and 5.9 °C (c1). Temperatures were higher in June 2020, ranging from 7.7 °C (c10) to 12.3 °C (c1) and in September 2020, ranging between 10.1 °C (c9) and 16.0 °C (c1). In June and September 2020, temperatures were more elevated in the shallower part of the basin.



230 **Figure 5.** (a) Diffusive CH<sub>4</sub> flux at the sediment-water interface of each campaign. The middle line of the boxes represent the median, the boxes demarcate the 25<sup>th</sup> and 75<sup>th</sup> percentiles, and the whiskers extend to the most extreme data points, not considering outliers. (b-c) Water temperature 0.5 m above the sediment (b) and the mean diffusive CH<sub>4</sub> flux (c) at each station of the transect with either one sediment core (indicated by black contour) or two sediment cores per station at each campaign (Error bars represent the range of values). The individual sampling stations are indicated above the panels.

## 235 4 Discussion

### 4.1 Seasonal and spatial differences in pore water CH<sub>4</sub> concentrations

240 CH<sub>4</sub> pore water concentrations in Schwarzenbach Reservoir ranged between 0.002 mmol L<sup>-1</sup> and 1.530 mmol L<sup>-1</sup>, which is comparable to what other studies have found in the sediment of freshwater systems (Schulz and Conrad, 1995; Murase and Sugimoto, 2001; Huttunen et al., 2006; Maeck et al., 2013; Noröi et al., 2013; Donis et al., 2017). The CH<sub>4</sub> pore water concentrations typically increased with increasing sediment depth (Fig. 3), which is consistent with observations in other studies (Frenzel et al., 1990; Huttunen et al., 2006; Deutzmann et al., 2014). The CH<sub>4</sub> pore water concentrations showed seasonal and spatial differences (Fig. 3). The median CH<sub>4</sub> concentration in the pore water across all measured profiles in September 2020 (0.68 mmol L<sup>-1</sup>) was almost two times larger than in June 2020 (0.37 mmol L<sup>-1</sup>) and about four times larger



than in April 2019 ( $0.16 \text{ mmol L}^{-1}$ ) (Fig. 3b). The increase in pore water concentration with the season may be explained by  
245 differences in  $\text{CH}_4$  production within the sediment. Many studies have demonstrated that  $\text{CH}_4$  production rates in sediments  
are enhanced at higher temperatures (Schulz et al., 1997; Lofton et al., 2014; Marotta et al., 2014; Shelley et al., 2015;  
Sepulveda-Jauregui et al., 2018). In Schwarzenbach Reservoir, sediment temperatures increased as the season progressed  
(Fig. 5b), supporting the hypothesis that higher production was responsible for larger pore water  $\text{CH}_4$  concentrations later in  
the season. Enhanced  $\text{CH}_4$  concentrations were present, especially in deeper sediment layers, which are stronger affected by  
250 changes in production and less affected by  $\text{CH}_4$  losses due to oxidation and vertical transport than the upper sediment layers.  
However, the spatial distributions of pore water  $\text{CH}_4$  along the transect during the different campaigns cannot be explained  
by temperature alone. Sediment temperatures were elevated in the shallow water zone in June and September 2020, but  $\text{CH}_4$   
concentrations were generally largest near the center of the transect and lowest towards the western and eastern end of the  
basin (Fig. 3a). Availability of organic matter in the sediment is another factor that correlates with  $\text{CH}_4$  production (Duc et  
255 al., 2010) or  $\text{CH}_4$  concentrations (Murase and Sugimoto, 2001) in lake sediments and is considered to be a major limiting  
factor for  $\text{CH}_4$  production (Segers, 1998). Settling of organic matter is known to correlate with the current velocity of the  
inflows (Kufel, 1991). Fewer organic particles might deposit close to the inflows than in the open water because water  
current velocity is likely to be smaller in the open water of the central basin than near the inflows.

#### 4.2 Significance of the potentially released amount of $\text{CH}_4$ due to reservoir flushing

260 Assuming that the  $\text{CH}_4$  stored in the sediment is completely released into the water during the sediment flushing process and  
degasses quickly to the atmosphere when the water is rapidly transported out of the reservoir,  $N_{\text{CH}_4, \text{FSL}}$  provides a measure of  
the potential  $\text{CH}_4$  emission from the reservoir due to flushing. The amount of  $\text{CH}_4$  mobilized during a flushing operation  
depends on the depth of sediment erosion and on the season (Fig. 4a). Flushing operation eroding a 15 cm thick sediment  
layer in the assumed 60 m wide flushing channel along the thalweg of Schwarzenbach Reservoir implies a flushed sediment  
265 volume of  $16.5 \times 10^3 \text{ m}^3$ , which agrees well with the study by Saam et al. (2019), who assessed the feasibility of reservoir  
flushing in Schwarzenbach and obtained a flushed sediment volume of  $13.6 \times 10^3 \text{ m}^3$  in a simulation of a full drawdown  
flushing scenario. At an erosion depth of 15 cm, the resulting  $N_{\text{CH}_4, \text{FSL}}$  are 6.5 kmol  $\text{CH}_4$ , 8.1 kmol  $\text{CH}_4$ , and 12.5 kmol  $\text{CH}_4$   
if the flushing operation is conducted in April, June, and September, respectively. This suggests that conducting a reservoir  
flushing operation in spring rather than in late summer would reduce flushing induced  $\text{CH}_4$  emissions in Schwarzenbach  
270 Reservoir by a factor of 2.

Typical  $\text{CH}_4$  emission pathways in Schwarzenbach Reservoir include  $\text{CH}_4$  emissions due to ebullition ( $212 \text{ mol d}^{-1}$   
during normal operation mode), diffusive  $\text{CH}_4$  emissions ( $27 \text{ mol d}^{-1}$ ), and  $\text{CH}_4$  emissions due to degassing during  
turbination ( $14 \text{ mol d}^{-1}$ ) (Peeters et al., 2019; Encinas Fernández et al., 2020). Together,  $\text{CH}_4$  emissions by these pathways  
add up to  $253 \text{ mol d}^{-1}$  or  $92.4 \text{ kmol yr}^{-1}$ . Hence, one flushing operation with 15 cm erosion depth potentially causes  $\text{CH}_4$   
275 emissions that would account for 7 (flushing in April) –14% (flushing in September) of the typical annual  $\text{CH}_4$  emission in  
Schwarzenbach Reservoir.



Not only the total amount of CH<sub>4</sub> but also the average CH<sub>4</sub> concentration in the flushed sediment increases with increasing erosion depth (Fig. 4b). This implies that overall less CH<sub>4</sub> is released if an equivalent sediment volume is eroded by several flushings mobilizing thin layers of sediment instead of a few flushings mobilizing thicker sediment layers. For instance, if flushing in April mobilizes the top 5 cm, 10 cm, or 100 cm of sediment,  $C_{CH_4,FSL}$  is 0.10 mmol L<sup>-1</sup>, 0.27 mmol L<sup>-1</sup>, and 0.74 mmol L<sup>-1</sup>, respectively (Fig. 4b and Fig. S2). Hence, the potential release of CH<sub>4</sub> during one flushing event of a 100 cm thick sediment layer is about 2.7 or 7.5, times, larger than 10 flushing events of 10 cm and 20 flushing events of 5 cm thick sediment layers, respectively. Below ~50 cm of sediment,  $C_{CH_4,FSL}$  is essentially constant (Fig. S2) and thus,  $N_{CH_4,FSL}$  in flushing events eroding more than 50 cm of sediment increases essentially linearly with the volume of sediment eroded.

Note, that Schwarzenbach Reservoir has been emptied so far only three times since its completion. However, many reservoirs worldwide are flushed regularly, such as the Dashidaira reservoir in Japan (storage capacity of  $9 \times 10^6$  m<sup>3</sup>), where a flushing operation with full water level drawdown is conducted annually (Esmaili et al., 2017; Sumi et al., 2017). In this reservoir, flushed sediment volumes between  $60 \times 10^3$  and  $590 \times 10^3$  m<sup>3</sup> with an average flushed sediment volume of  $287 \times 10^3$  m<sup>3</sup> have been reported (Sumi et al., 2009; Esmaili et al., 2017). Therefore, the average flushed sediment volume in Dashidaira reservoir is 17–21 times larger than the estimated flushed sediment volumes in the study of Saam et al. (2019) and in this study.

Unfortunately, no data is available on CH<sub>4</sub> concentration in the sediment or CH<sub>4</sub> emissions of Dashidaira reservoir. However, assuming that CH<sub>4</sub> concentrations in the sediment of Dashidaira reservoir are comparable to those in Schwarzenbach Reservoir and that the erosion depth is 100 cm or more, the average concentration in the flushed sediment can be approximated by  $C_{CH_4,FSL}$  of 0.73 mol m<sup>-3</sup>, which is the average CH<sub>4</sub> concentrations in the sediment flushed layer at 100 cm erosion depth in Schwarzenbach reservoir (Fig. S2). Therefore, the average flushed sediment volume in Dashidaira reservoir of  $287 \times 10^3$  m<sup>3</sup>, would contain 210 kmol CH<sub>4</sub>. Because the reservoir is flushed each year, the emissions from this reservoir due to flushing would be ~210 kmol yr<sup>-1</sup>, i.e., 2.3 times larger than the typical annual emissions from Schwarzenbach Reservoir. Hence, CH<sub>4</sub> emissions due to reservoir flushing operations can contribute substantially to overall CH<sub>4</sub> emissions from reservoirs.

CH<sub>4</sub> emissions due to reservoir flushing can represent a significant contributing pathway to overall CH<sub>4</sub> emissions from reservoirs only if CH<sub>4</sub> production in the sediment can provide the amount of CH<sub>4</sub> in the flushed sediment volumes between flushing operations. In Schwarzenbach Reservoir, the measured CH<sub>4</sub> flux at the sediment-water interface was 1.02 mmol m<sup>-2</sup> d<sup>-1</sup> (average over all measurements). Typically, 60–90% of CH<sub>4</sub> produced in the sediment is oxidized (Le Mer and Roger, 2001). To compensate the flux from the sediment and the loss due to oxidation of the produced CH<sub>4</sub> requires a CH<sub>4</sub> production per unit sediment surface of 2.6–10.2 mmol m<sup>-2</sup> d<sup>-1</sup>. Considering a 100 cm thick layer of sediment, this implies a CH<sub>4</sub> production of 2.6–10.2 mmol m<sup>-3</sup> d<sup>-1</sup>. This estimated production rate is compatible with the median production rate of 10 mmol m<sup>-3</sup> d<sup>-1</sup> obtained from direct measurements of production rates in sediments of lakes (the median of a data compilation of 93 samples of different lake sediments; (Martinez-Cruz et al., 2018)). At a CH<sub>4</sub> production rate of 2.6–10.2 mmol m<sup>-3</sup> d<sup>-1</sup>, the time required to produce the average CH<sub>4</sub> concentration in the flushed sediment  $C_{CH_4,FSL} = 0.73$  mol m<sup>-3</sup> is



73–291 days. This estimation suggests that CH<sub>4</sub> production in the sediments provides sufficient CH<sub>4</sub> in the flushed sediment layers between annual flushing operations.

#### 4.3 Additional indirect CH<sub>4</sub> emissions due to reservoir flushing

315 CH<sub>4</sub> emissions due to reservoir flushing might be not only limited to the direct CH<sub>4</sub> emissions (i.e., when sediment is eroded and the stored CH<sub>4</sub> is released to the water column and eventually into the atmosphere), but a flushing operation might also cause additional indirect CH<sub>4</sub> emissions. During a drawdown flushing operation, the water is released through one or more outlets and the water level is decreased dramatically, resulting in an additional drawdown flux, as the stored CH<sub>4</sub> in the water column can degas during turbination. Furthermore, as water level fluctuations in reservoirs can enhance CH<sub>4</sub> ebullition due to changing hydrostatic pressure (Harrison et al., 2017; Encinas Fernández et al., 2020), lowering the water level during the drawdown period would cause an additional CH<sub>4</sub> ebullition flux. While this also reduces the amount of CH<sub>4</sub> in the sediment accessible to the emissions due to sediment erosion, the total emission due to reservoir flushing might still be higher, as CH<sub>4</sub> production in the sediment could partly replace the CH<sub>4</sub> that was lost due to ebullition for the duration of the drawdown period. Lastly, it was shown that the CH<sub>4</sub> flux from sediments can be enhanced for several days when they fall dry (Kosten et al., 2018), thus leading to additional CH<sub>4</sub> emissions due to exposed sediment areas during the flushing operation.

#### 325 5 Conclusions

Assessing the significance of CH<sub>4</sub> emissions due to reservoir flushing in comparison to other pathways requires consideration of the flushing frequency, the flushed sediment volume, the erosion depth during the flushing event, and the vertical and lateral distribution of CH<sub>4</sub> concentrations in the sediment. In Schwarzenbach Reservoir, we estimated that one flushing operation could potentially cause CH<sub>4</sub> emissions that are comparable to 7–14% of the reservoir's typical annual emissions. Seasonal differences in CH<sub>4</sub> concentrations in the sediment suggest that the timing of the flushing operation during the season affects the amount of CH<sub>4</sub> emitted. Because the CH<sub>4</sub> concentration increases with depth in the sediment, removal of the same sediment volume by regular flushing of shallow sediment layers causes less CH<sub>4</sub> emissions than few flushings of thicker sediment layers. In Schwarzenbach Reservoir, flushing is not conducted regularly. However, there are many reservoirs where flushing operations mobilize much larger volumes of sediment and are conducted more regularly than in Schwarzenbach Reservoir. In these reservoirs, CH<sub>4</sub> emission due to reservoir flushing is likely substantial, and thus their overall CH<sub>4</sub> emission might be severely underestimated.

#### Author contribution

OL: Conceptualization, Formal analysis, Investigation, Project administration, Software, Visualization, Writing – original draft, Writing – review & editing. JEF: Investigation, Project administration, Writing – review & editing. KMC: Resources,



340 Writing – review & editing, FP: Conceptualization, Formal analysis, Funding acquisition, Project administration, Resources, Software, Supervision, Writing – review & editing.

### Acknowledgements

We thank Enzo Gronchi, Ramona Ragg, Raymund Hackett, Louis Lauber and Beatrix Rosenberg for technical assistance in the field, and we are grateful to the members of our group for valuable feedback in the early stage of the article.

### 345 Financial Support

This work was financially supported by the Ministry of Science, Research and the Arts of the Federal State Baden-Württemberg, Germany (Grant: Water Research Network project: Challenges of Reservoir Management – Meeting Environmental and Social Requirements).

### References

- 350 Antoine, G., Camenen, B., Jodeau, M., Némery, J., and Esteves, M.: Downstream erosion and deposition dynamics of fine suspended sediments due to dam flushing, *J. Hydrol.*, 585, 124763, <https://doi.org/10.1016/j.jhydrol.2020.124763>, 2020.
- Bastviken, D., Ejlertsson, J., and Tranvik, L.: Measurement of methane oxidation in lakes: A comparison of methods, *Environ. Sci. Technol.*, 36, 3354–3361, <https://doi.org/10.1021/es010311p>, 2002.
- Bastviken, D., Tranvik, L. J., Downing, J., Crill, J. a, M, P., and Enrich-prast, A.: Freshwater Methane Emissions Offset the  
355 Continental Carbon Sink, *Science.*, 331, 50, <https://doi.org/10.1126/science.1196808>, 2011.
- Berner, R. A.: *Early Diagenesis: a Theoretical Approach*, Princeton Univ. Press, 1980.
- Boudreau, B. P.: *Diagenetic Models and Their Implementation: Modelling Transport and Reactions in Aquatic Sediments*, 505, Springer, Berlin, Germany, pp. 436, 1997.
- Brandt, S. A. and Swenning, J.: Sedimentological and geomorphological effects of reservoir flushing: The Cachi reservoir,  
360 Costa Rica, 1996, *Geogr. Ann. Ser. A, Phys. Geogr.*, 81, 391–407, <https://doi.org/10.1111/j.0435-3676.1999.00069.x>, 1999.
- Brimhall, G. H. and Dietrich, W. E.: Constitutive mass balance relations between chemical composition, volume, density, porosity, and strain in metasomatic hydrochemical systems: Results on weathering and pedogenesis, *Geochim. Cosmochim. Acta*, 51, 567–587, [https://doi.org/10.1016/0016-7037\(87\)90070-6](https://doi.org/10.1016/0016-7037(87)90070-6), 1987.
- Chang, F., Lai, J., and Kao, L.: Optimization of operation rule curves and flushing schedule in a reservoir, *Hydrol. Process.*,  
365 17, 1623–1640, <https://doi.org/10.1002/hyp.1204>, 2003.
- Chanton, J. P. and Whiting, G. J.: Trace gas exchange in freshwater and coastal marine environments: ebullition and transport by plants, *Biog. trace gases Meas. Emiss. from soil water*, Blackwell Publishing, 98–125, 1995.



- Deemer, B. R., Harrison, J. A., Li, S., Beaulieu, J. J., DelSontro, T., Barros, N., Bezerra-Neto, J. F., Powers, S. M., dos Santos, M. A., and Vonk, J. A.: Greenhouse Gas Emissions from Reservoir Water Surfaces: A New Global Synthesis, *Bioscience*, 66, 949–964, <https://doi.org/10.1093/biosci/biw117>, 2016.
- 370 DelSontro, T., McGinnis, D. F., Sobek, S., Ostrovsky, I., and Wehrli, B.: Extreme methane emissions from a Swiss hydropower reservoir: contribution from bubbling sediments, *Environ. Sci. Technol.*, 44, 2419–2425, <https://doi.org/10.1021/es9031369>, 2010.
- Deutzmann, J. S., Stief, P., Brandes, J., and Schink, B.: Anaerobic methane oxidation coupled to denitrification is the dominant methane sink in a deep lake, *Proc. Natl. Acad. Sci.*, 111, 18273–18278, <https://doi.org/10.1073/pnas.1411617111>, 2014.
- 375 Donis, D., Flury, S., Stöckli, A., Spangenberg, J. E., Vachon, D., and McGinnis, D. F.: Full-scale evaluation of methane production under oxic conditions in a mesotrophic lake, *Nat. Commun.*, 8, 1–11, <https://doi.org/10.1038/s41467-017-01648-4>, 2017.
- 380 Duc, N. T., Crill, P., and Bastviken, D.: Implications of temperature and sediment characteristics on methane formation and oxidation in lake sediments, *Biogeochemistry*, 100, 185–196, <https://doi.org/10.1007/s10533-010-9415-8>, 2010.
- Encinas Fernández, J., Peeters, F., and Hofmann, H.: Importance of the Autumn Overturn and Anoxic Conditions in the Hypolimnion for the Annual Methane Emissions from a Temperate Lake, *Environ. Sci. Technol.*, 48, 7297–7304, <https://doi.org/10.1021/es4056164>, 2014.
- 385 Encinas Fernández, J., Hofmann, H., and Peeters, F.: Diurnal pumped-storage operation minimizes methane ebullition fluxes from hydropower reservoirs, *Water Resour. Res.*, 56, e2020WR027221, <https://doi.org/10.1029/2020WR027221>, 2020.
- Esmaeili, T., Sumi, T., Kantoush, S. A., Kubota, Y., Haun, S., and Rütther, N.: Three-dimensional numerical study of free-flow sediment flushing to increase the flushing efficiency: a case-study reservoir in Japan, *Water*, 9, 900, [10.3390/w9110900](https://doi.org/10.3390/w9110900), 2017.
- 390 Frenzel, P., Thebrath, B., and Conrad, R.: Oxidation of methane in the oxic surface layer of a deep lake sediment (Lake Constance), *FEMS Microbiol. Lett.*, 73, 149–158, [https://doi.org/10.1016/0378-1097\(90\)90661-9](https://doi.org/10.1016/0378-1097(90)90661-9), 1990.
- Fruchard, F. and Camenen, B.: Reservoir sedimentation: different type of flushing-friendly flushing example of genissiat dam flushing, in: *ICOLD International Symposium on Dams for a changing world*, 6-p, 2012.
- Grimardias, D., Guillard, J., and Cattaneo, F.: Drawdown flushing of a hydroelectric reservoir on the Rhône River: Impacts on the fish community and implications for the sediment management, *J. Environ. Manage.*, 197, 239–249, <https://doi.org/10.1016/j.jenvman.2017.03.096>, 2017.
- 395 Harrison, J. A., Deemer, B. R., Birchfield, M. K., and O'Malley, M. T.: Reservoir Water-Level Drawdowns Accelerate and Amplify Methane Emission, *Environ. Sci. Technol.*, 51, 1267–1277, <https://doi.org/10.1021/acs.est.6b03185>, 2017.
- Hoffert, M. I., Caldeira, K., Jain, A. K., Haites, E. F., Harvey, L. D. D., Potter, S. D., Schlesinger, M. E., Schneider, S. H., Watts, R. G., Wigley, T. M. L., and Wuebbles, D. J.: Energy implications of future stabilization of atmospheric CO<sub>2</sub> content, *Nature*, 395, 881–884, <https://doi.org/10.1038/27638>, 1998.
- 400



- Hofmann, H., Federwisch, L., and Peeters, F.: Wave-induced release of methane: Littoral zones as a source of methane in lakes, *Limnol. Oceanogr.*, 55, 1990–2000, <https://doi.org/10.4319/lo.2010.55.5.1990>, 2010.
- Huttunen, J. T., Väisänen, T. S., Hellsten, S. K., and Martikainen, P. J.: Methane fluxes at the sediment-water interface in some boreal lakes and reservoirs, *Boreal Environ. Res.*, 11, 27–34, 2006.
- ICOLD, C.: Sedimentation and sustainable use of reservoir and river systems, Draft ICOLD Bull. Sediment. Comm., 2009.
- Kantoush, S., Sumi, T., Suzuki, T., and Murasaki, M.: Impacts of sediment flushing on channel evolution and morphological processes: Case study of the Kurobe River, Japan, *River Flow 2010*, 1165–1176, 2010.
- Kantoush, S. A. and Sumi, T.: River morphology and sediment management strategies for sustainable reservoir in Japan and European Alps, *Disaster Prevention Research Institute Annuals, Kyoto Univ.*, 53, 821–839, 2010.
- Kemenes, A., Forsberg, B. R., and Melack, J. M.: Methane release below a tropical hydroelectric dam, *Geophys. Res. Lett.*, 34, L12809, <https://doi.org/10.1029/2007GL029479>, 2007.
- Kosten, S., van den Berg, S., Mendonça, R., Paranaíba, J. R., Roland, F., Sobek, S., Van Den Hoek, J., and Barros, N.: Extreme drought boosts CO<sub>2</sub> and CH<sub>4</sub> emissions from reservoir drawdown areas, *Inl. Waters*, 8, 329–340, <https://doi.org/10.1080/20442041.2018.1483126>, 2018.
- Kufel, L.: Nutrient sedimentation at the river inflow to a lake, *SIL Proceedings, 1922-2010*, 24, 1772–1774, <https://doi.org/10.1080/03680770.1989.11899069>, 1991.
- Lehner, B., Liermann, C. R., Revenga, C., Vörösmarty, C., Fekete, B., Crouzet, P., Döll, P., Endejan, M., Frenken, K., Magome, J., Nilsson, C., Robertson, J. C., Rödel, R., Sindorf, N., and Wisser, D.: High-resolution mapping of the world's reservoirs and dams for sustainable river-flow management, *Front. Ecol. Environ.*, 9, 494–502, <https://doi.org/10.1890/100125>, 2011.
- Lofton, D. D., Whalen, S. C., and Hershey, A. E.: Effect of temperature on methane dynamics and evaluation of methane oxidation kinetics in shallow Arctic Alaskan lakes, *Hydrobiologia*, 721, 209–222, <https://doi.org/10.1007/s10750-013-1663-x>, 2014.
- St. Louis, V. L., Kelly, C. A., Duchemin, É., Rudd, J. W. M., and Rosenberg, D. M.: Reservoir Surfaces as Sources of Greenhouse Gases to the Atmosphere: A Global Estimate: Reservoirs are sources of greenhouse gases to the atmosphere, and their surface areas have increased to the point where they should be included in global inventories of, *Bioscience*, 50, 766–775, 10.1641/0006-3568(2000)050[0766:RSASOG]2.0.CO;2, 2000.
- Maeck, A., Delsontro, T., McGinnis, D. F., Fischer, H., Flury, S., Schmidt, M., Fietzek, P., and Lorke, A.: Sediment trapping by dams creates methane emission hot spots, *Environ. Sci. Technol.*, 47, 8130–8137, <https://doi.org/10.1021/es4003907>, 2013.
- Maeck, A., Hofmann, H., and Lorke, A.: Pumping methane out of aquatic sediments—ebullition forcing mechanisms in an impounded river, *Biogeosciences*, 11, 2925–2938, <https://doi.org/10.5194/bg-11-2925-2014>, 2014.
- Marotta, H., Pinho, L., Gudasz, C., Bastviken, D., Tranvik, L. J., and Enrich-Prast, A.: Greenhouse gas production in low-latitude lake sediments responds strongly to warming, *Nat. Clim. Chang.*, 4, 467–470, <https://doi.org/10.1038/nclimate2222>,





- 2014.
- Martinez-Cruz, K., Sepulveda-Jauregui, A., Casper, P., Anthony, K. W., Smemo, K. A., and Thalasso, F.: Ubiquitous and significant anaerobic oxidation of methane in freshwater lake sediments, *Water Res.*, 144, 332–340, <https://doi.org/10.1016/j.watres.2018.07.053>, 2018.
- 440 Le Mer, J. and Roger, P.: Production, oxidation, emission and consumption of methane by soils: a review, *Eur. J. Soil Biol.*, 37, 25–50, [https://doi.org/10.1016/S1164-5563\(01\)01067-6](https://doi.org/10.1016/S1164-5563(01)01067-6), 2001.
- Morris, G. L.: Classification of management alternatives to combat reservoir sedimentation, *Water*, 12, 861, <https://doi.org/10.3390/w12030861>, 2020.
- Mouris, K., Beckers, F., and Haun, S.: Three-dimensional numerical modeling of hydraulics and morphodynamics of the Schwarzenbach reservoir, in: *E3S Web of Conferences*, 3005, 2018.
- 445 Murase, J. and Sugimoto, A.: Spatial distribution of methane in the Lake Biwa sediments and its carbon isotopic compositions, *Geochem. J.*, 35, 257–263, <https://doi.org/10.2343/geochemj.35.257>, 2001.
- Norði, K. à., Thamdrup, B., and Schubert, C. J.: Anaerobic oxidation of methane in an iron-rich Danish freshwater lake sediment, *Limnol. Oceanogr.*, 58, 546–554, <https://doi.org/10.4319/lo.2013.58.2.0546>, 2013.
- 450 Peeters, F., Encinas Fernandez, J., and Hofmann, H.: Sediment fluxes rather than oxic methanogenesis explain diffusive CH<sub>4</sub> emissions from lakes and reservoirs, *Sci. Rep.*, 9, 1–10, <https://doi.org/10.1038/s41598-018-36530-w>, 2019.
- Petkovšek, G., Roca, M., and Kitamura, Y.: Sediment flushing from reservoirs: a review, *Dams Reserv.*, 30, 12–21, <https://doi.org/10.1680/jdare.20.00005>, 2020.
- Ragg, R. B., Peeters, F., Ingwersen, J., Teiber-Siessegger, P., and Hofmann, H.: Interannual Variability of Methane Storage and Emission During Autumn Overturn in a Small Lake, *J. Geophys. Res. Biogeosciences*, 126, e2021JG006388, <https://doi.org/10.1029/2021JG006388>, 2021.
- Rosentreter, J. A., Borges, A. V., Deemer, B. R., Holgerson, M. A., Liu, S., Song, C., Melack, J., Raymond, P. A., Duarte, C. M., Allen, G. H., Olefeldt, D., Poulter, B., Battin, T. I., and Eyre, B. D.: Half of global methane emissions come from highly variable aquatic ecosystem sources, *Nat. Geosci.*, 14, 225–230, <https://doi.org/10.1038/s41561-021-00715-2>, 2021.
- 460 Saam, L., Mouris, K., Wieprecht, S., and Haun, S.: Three-dimensional numerical modelling of reservoir flushing to obtain long-term sediment equilibrium, in: *Proceedings of the 38th IAHR World Congress (Panama)*, Panama City, Panama, 1–6, 10.3850/38WC092019-0742, 2019.
- Schulz, S. and Conrad, R.: Effect of algal deposition on acetate and methane concentrations in the profundal sediment of a deep lake (Lake Constance), *FEMS Microbiol. Ecol.*, [https://doi.org/10.1016/0168-6496\(94\)00088-E](https://doi.org/10.1016/0168-6496(94)00088-E), 1995.
- 465 Schulz, S., Matsuyama, H., and Conrad, R.: Temperature dependence of methane production from different precursors in a profundal sediment (Lake Constance), *FEMS Microbiol. Ecol.*, 22, 207–213, <https://doi.org/10.1111/j.1574-6941.1997.tb00372.x>, 1997.
- Segers, R.: Methane production and methane consumption: a review of processes underlying wetland methane fluxes, *Biogeochemistry*, 41, 23–51, <https://doi.org/10.1023/A:1005929032764>, 1998.



- 470 Sepulveda-Jauregui, A., Hoyos-Santillan, J., Martinez-Cruz, K., Walter Anthony, K. M., Casper, P., Belmonte-Izquierdo, Y.,  
and Thalasso, F.: Eutrophication exacerbates the impact of climate warming on lake methane emission, *Sci. Total Environ.*,  
636, 411–419, <https://doi.org/10.1016/j.scitotenv.2018.04.283>, 2018.
- Shelley, F., Abdullahi, F., Grey, J., and Trimmer, M.: Microbial methane cycling in the bed of a chalk river: oxidation has  
the potential to match methanogenesis enhanced by warming, *Freshw. Biol.*, 60, 150–160,  
475 <https://doi.org/10.1111/fwb.12480>, 2015.
- Sobek, S., DelSontro, T., Wongfun, N., and Wehrli, B.: Extreme organic carbon burial fuels intense methane bubbling in a  
temperate reservoir, *Geophys. Res. Lett.*, 39, <https://doi.org/10.1029/2011GL050144>, 2012.
- Sumi, T., Nakamura, S., and Hayashi, K.: The effect of sediment flushing and environmental mitigation measures in the  
Kurobe River, in: 23rd ICOLD Congress, 2009.
- 480 Sumi, T., Kantoush, S., Esmaili, T., and Ock, G.: Reservoir sediment flushing and replenishment below dams: insights from  
Japanese case studies, *Gravel-Bed Rivers Process. Disasters*, 385–414, <https://doi.org/10.1002/9781118971437.ch14>, 2017.
- Wanninkhof, R.: Relationship between wind speed and gas exchange over the ocean, *J. Geophys. Res. Ocean.*, 97, 7373–  
7382, <https://doi.org/10.1029/92JC00188>, 1992.
- WCD (World Commission on Dams): Dams and development: A new framework for decision-making: The report of the  
485 world commission on dams, Earthscan, 2000.
- Weast, R. C.: *CRC Handbook of Chemistry and Physics*, 69th ed., F-37-F-40 pp., 1988.
- Zarfl, C., Lumsdon, A. E., Berlekamp, J., Tydecks, L., and Tockner, K.: A global boom in hydropower dam construction,  
*Aquat. Sci.*, 77, 161–170, <https://doi.org/10.1007/s00027-014-0377-0>, 2015.